MSE6701H - Multiscale Materials Modeling and Simulation

Modeling the melting behaviour of Pure Ni, Zr, and Ni-Zr Alloys: A Computational Study

Technical Report

Luigi Casagrande (J12405099002)

1 December 2024

Contents

1 Introduction

Advanced materials play a critical role in modern engineering, enabling the development of systems and components capable of withstanding extreme conditions and demanding performance requirements. Transition metals, with their versatile properties and ability to form alloys and intermetallic compounds, are foundational to this progress.

Among these, nickel (Ni) and zirconium (Zr) stand out due to their exceptional mechanical, thermal, and chemical characteristics, making them indispensable in diverse applications ranging from aerospace to energy systems.

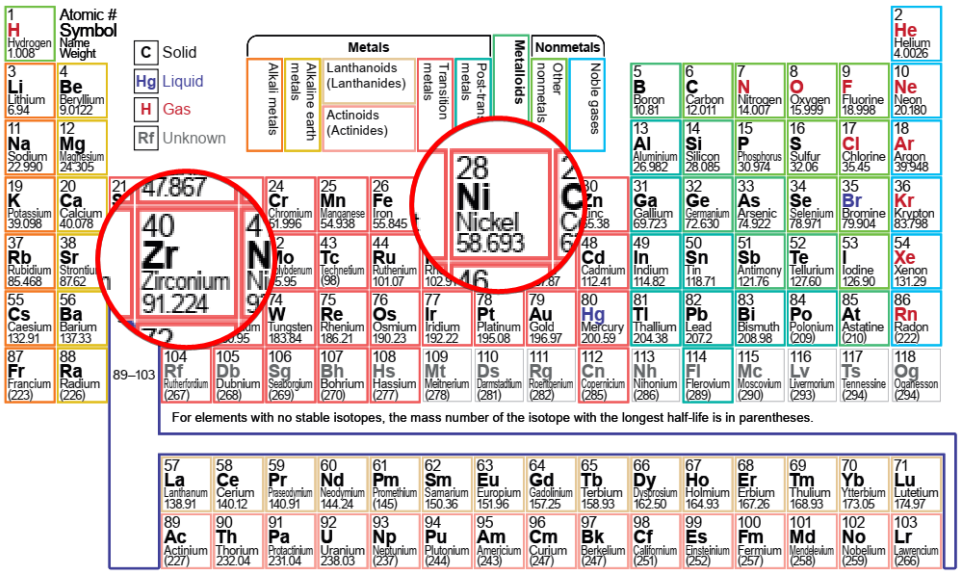

Figure 1: Periodic Table highlighting the Ni and Zr elements. [1]

Nickel (Ni) is a transition metal with notable mechanical and chemical properties; it crystallizes in a face-centered cubic (FCC) lattice, which provides excellent ductility, toughness, and a high degree of slip systems during deformation.

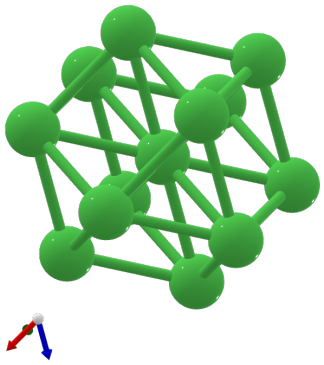

Figure 2: Ni crystallizes in the cubic $Fm\bar{3}m$ space group. [2]

Its melting point, approximately 1455 °C, is indicative of strong metallic bonding, and

its chemical inertness lends itself to superior corrosion resistance. These characteristics make nickel a vital component in high-performance materials such as superalloys, battery electrodes, and catalysts [3].

Zirconium (Zr) is another transition metal known for its unique combination of chemical and mechanical properties. It exhibits a hexagonal close-packed (HCP) crystal structure at room temperature, transitioning to a body-centered cubic (BCC) structure above 863 °C.

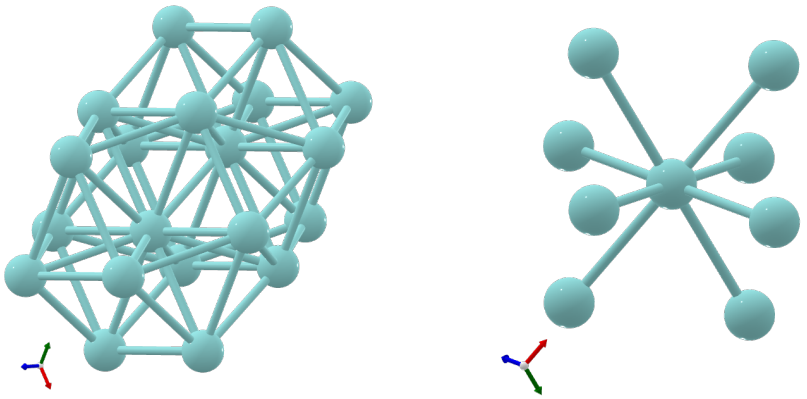

(a) Zr crystallizes in the hexagonal $P6_3/mmc$ space group.

(b) Zr crystallizes in the cubic $Im\bar{3}m$ space group.

Figure 3: Different Zr crystallizations based on the temperature. [2]

Zirconium's melting point is approximately 1855 °C, and it is well-regarded for its outstanding resistance to corrosion in aggressive environments, including acidic and nuclear reactor conditions. Its low neutron absorption cross-section further makes it indispensable in nuclear engineering, especially for cladding materials in reactors [4].

Nickel (Ni), zirconium (Zr), and their alloys are widely used in catalysis, where Ni/Zr-mediated systems have facilitated efficient organic synthesis, such as ketone coupling for complex molecule production [5]. Those catalysts, including unsupported layered double hydroxides, show promise in industrial chemical processes due to their superior stability and activity. Materials like bimetallic sulphide films ($NiZr_2S_4$) and $Ni{-}Cr{-}ZrO_2$ coatings improve tribological performance, corrosion resistance, and wear resistance, making them ideal for structural and industrial applications [6].

In biomedicine, Ni-Zr metallic glasses and substituted magnetic materials offer advanced electronic and magnetic properties for energy storage and device applications [7]. Additionally, the system is pivotal in hydrogen storage technologies, as Ni-Zr intermetallic compounds like Zr_2Ni and Zr_2Ni_7 demonstrate excellent hydrogen solubility [8].

1.1 Ni-Zr Phase Diagram

The Ni-Zr system is a well-studied binary alloy system that exhibits a variety of stable intermetallic phases, each with distinct stoichiometries and crystal structures, as seen in Figure 4.

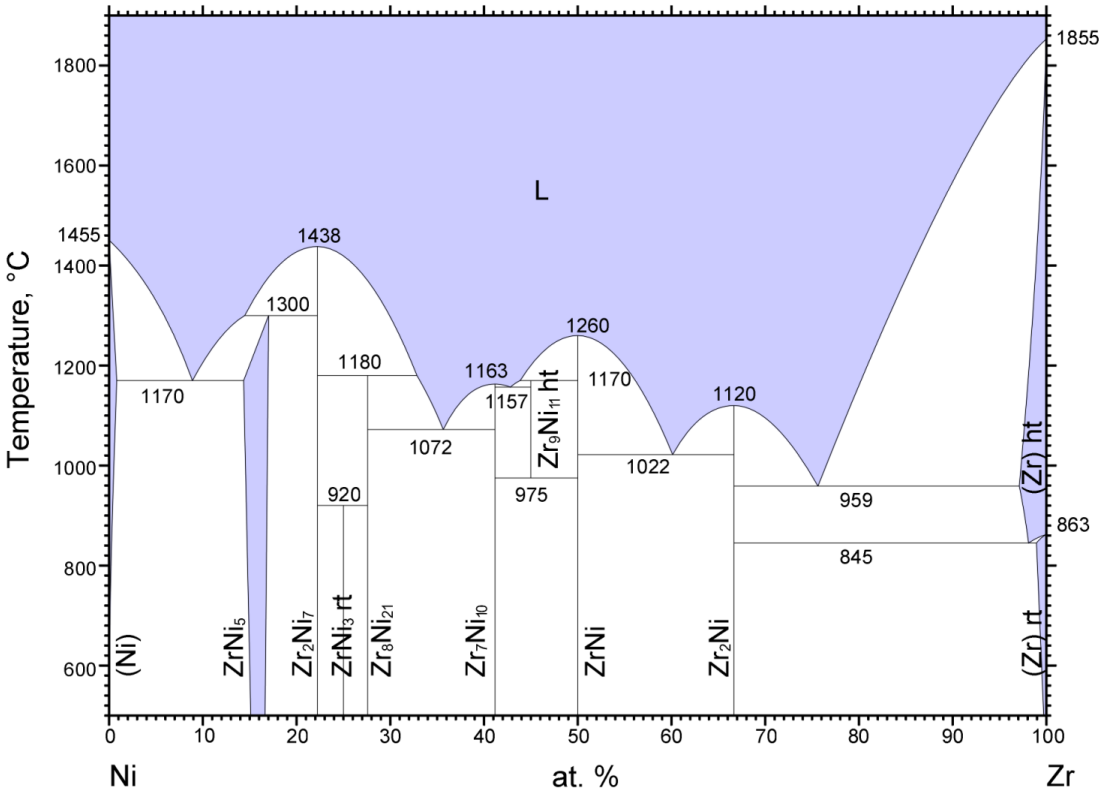

Figure 4: NiZr Phase Diagram. [9]

At the core of the Ni-Zr phase diagram are three important intermetallic compounds: ZrNi, Zr_2Ni, and Zr_2Ni_7. These phases are defined by their specific compositions and unique crystal structures, which impart distinct properties.
The stability of these phases arises from their thermodynamically favorable formation energies and the strong metallic bonding between Ni and Zr atoms.

- **ZrNi Phase:** it has a composition of 50 at.% Zr and 50 at.% Ni, crystallizes in an orthorhombic structure (space group *Cmcm*). This phase is highly valued for its excellent thermal stability and mechanical strength, making it well-suited for high-temperature and wear-resistant applications. Its ordered lattice minimizes defects, enhancing hardness and resistance to creep under stress. The melting point of this phase is 1260 °C [10,11].

- **Zr_2Ni Phase:** it is composed of 66.7 at.% Zr and 33.3 at.% Ni, adopts a tetragonal structure (space group *I4/mcm*). Known for its high wear resistance and moderate

toughness, this phase is commonly utilized in coatings and composite materials to improve durability. The melting point of this phase is 1120 °C [10,11].

- **Zr_2Ni_7 Phase:** with 22.2 at.% Zr and 77.8 at.% Ni, features a monoclinic structure (space group $P2_1/c$) and is distinguished by its exceptional hydrogen absorption properties. This makes Zr_2Ni_7 particularly relevant for energy storage applications. The melting point of this intermetallic phase is 1438 °C [11].

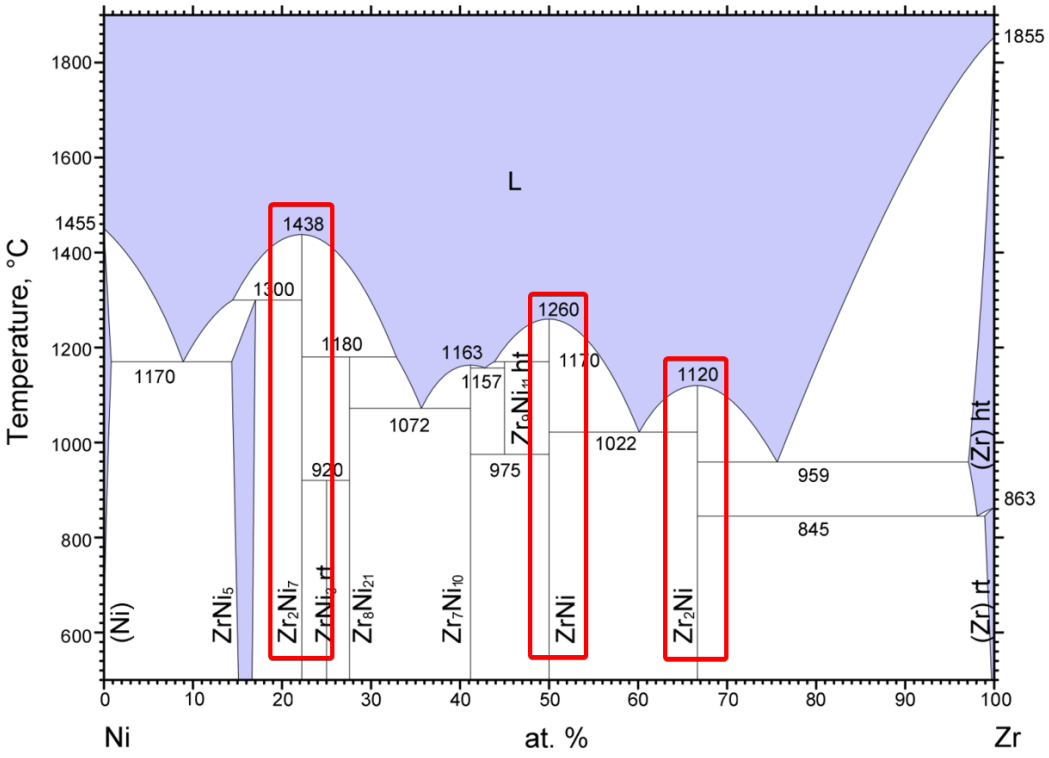

Figure 5: Highlight of the intermetallic compounds under examination. [9]

2 Computational methods

To ensure clarity and efficient data management throughout the simulation process, the files inside the cluster were organized into a structured hierarchy under a main directory named `'HW4-MD'` (as seen in Figure 6 and also in the `.zip` attached to this document).

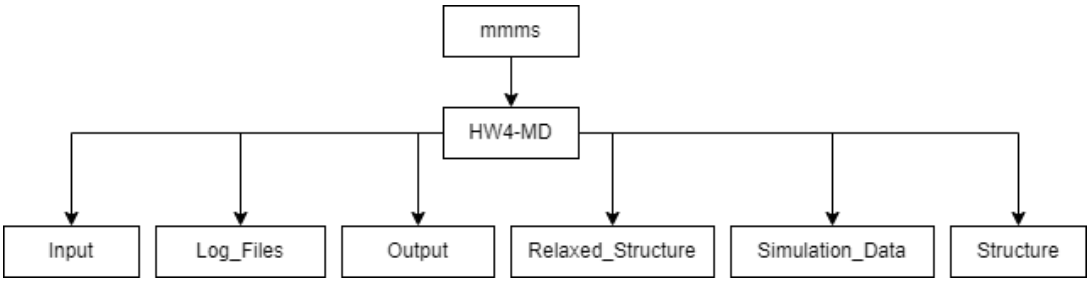

Figure 6: Folder organization for this work.

Within this directory, five subfolders were created, each dedicated to a specific type of file or function:

- `Input` ▸ This folder contains all input scripts and configuration files used for running the melting simulations in LAMMPS
- `Log_Files` ▸ All log files generated during the simulations are stored here
- `Output` ▸ This folder is used to store simulation results formatted for visualization in OVITO, so phase formation and melting processes (as seen in section 2.3 and 2.4)
- `Relaxed_Structure` ▸ This folder contain the LAMMPS code for the relaxation of the original material, provided from the `'Structure'` folder
- `Simulation_Data` ▸ Data files required for or generated by post-processing are placed in this folder. This includes information for further analysis in external software for calculating melting temperatures; MATLAB was used in this study
- `Structure` ▸ This folder contains structure files defining the initial atomic arrangements of the crystals

It is important to note that the run files are not included in the attached `.zip` file. However, to ensure proper execution of the simulation, the run files must be executed from within the `'Input'` folder, as all output data is referenced from that location. Further details regarding this process can be found in sections 2.3 and 2.4 of this report.

The naming convention for all files follows a systematic structure: each file name begins with the compound name, followed by the scope of the file (e.g., for a dump file related to the two-phase creation process the name is `'Zr2Ni7-two_phase_creation.dump'`).

Input files are prefixed with `'in.'`, log files are prefixed with `'log-'`, and other files are named according to their specific role in the simulation.

2.1 Potential Model

Despite the extensive study of Ni-Zr alloys due to their technological importance, the availability of robust potential energy functions for accurately modeling their thermodynamic properties remains limited.

The potential file for Ni-Zr alloys employed in this study was developed by S.R. Wilson and M.I. Mendelev [12] (file name `'Ni-Zr.eam.fs'`). It is an updated version of the 2012 potential (Mikhail Mendelev, Ames Laboratory) [13] and was specifically designed to *"simulate the solidification of Ni-Zr alloys, focusing on the B2, B33, and C16 phases"*.
This potential provides a reliable basis for modeling the interactions within Ni-Zr systems, but it is optimized for simulating processes like solidification, leaving gaps when modeling phase transitions such as melting with steady and linear heating procedure.
To overcome this limitation, a different approach was required to adapt the existing potential energy models for determining more accurately the melting temperatures of the intermetallic alloys (section 2.3).

The potential file used for pure Ni was originally developed by G.J. Ackland, G. Tichy, V. Vitek, and M.W. Finnis in 1987 [14]. It was subsequently converted to the `EAM/fs` format by M.I. Mendelev in 2009 (file name `'Ni_v1.eam.fs'`). In 2017, G.J. Ackland further refined the potential to incorporate close-range repulsion, specifically for radiation studies (file name `'Ni_v2.eam.fs'`) [15].
The most accurate potential is the latest `v2` version, but in this analysis, both files were included to demonstrate the reproducibility of the LAMMPS script and the limitations imposed from the usage of a wrong potential file (as seen in section 3.4).

The potential file used for Zr was developed by M.I. Mendelev and G.J. Ackland in 2007 [16] (file name `'Zr.eam.fs'`) [17]. It was primarily designed for the study of Zr in the solid state.

All these potentials are based on the Finnis-Sinclair (FS) formalism [14], a subset of the Embedded Atom Method (EAM). FS potentials are widely used in molecular dynamics simulations to describe metallic systems due to their ability to incorporate the many-body interactions characteristic of metallic bonding.

In the FS model, the total potential energy of the system U_{total} is expressed as:

$$U_{\text{total}} = \sum_i F\left(\rho_i\right) + \frac{1}{2}\sum_{i \neq j} \phi_{ij}\left(r_{ij}\right)$$

where $F(\rho_i)$ is the embedding energy, representing the energy required to place an atom i in the local electron density ρ_i generated by surrounding atoms, $\phi_{ij}(r_{ij})$ is the pairwise interaction potential between atoms i and j, which depends on the interatomic distance r_{ij}, while ρ_i is the local electron density at atom i, contributed by neighboring atoms.

This formulation captures two critical aspects of metallic systems:

1. Many-body effects: The embedding function $F(\rho_i)$ reflects the cohesive energy resulting from the collective electronic environment around an atom, which cannot be captured by simple pairwise potentials.

2. Bonding flexibility: The pairwise term ϕ_{ij} ensures accurate modeling of short-range atomic interactions, such as repulsion at small distances.

2.2 Inputs Creation

For each of the five compounds, two files were generated:

1. Single Cell File: This file contains the atomic structure of the single primitive cell, which defines the crystal base (`.poscar` file format). It serves as the foundational structure for generating a larger system (Figure 7).
   These files were extracted from the Materials Project database [2].

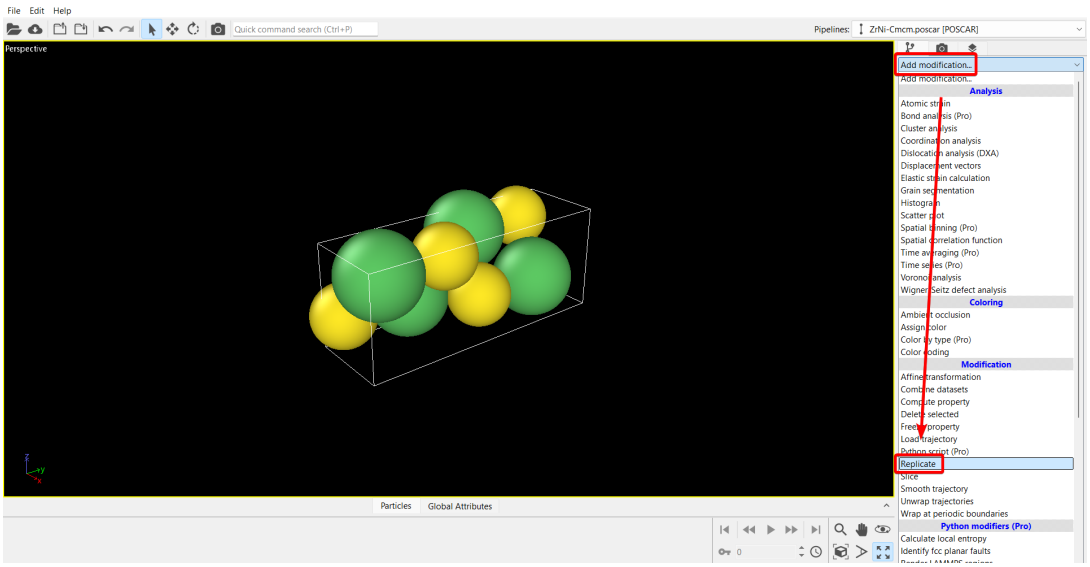

Figure 7: Single cell to replicate along the axis.

2. Bulk Material File: The second file represents the bulk material, which was obtained by replicating the single cell along the x, y, and z directions using the `'replicate'` modification in OVITO. This replication process expanded the system, mimicking a bulk material suitable for simulating phase transitions and material properties.

After replication, the bulk structure was exported into a LAMMPS-compatible file format, as shown in Figure 8.

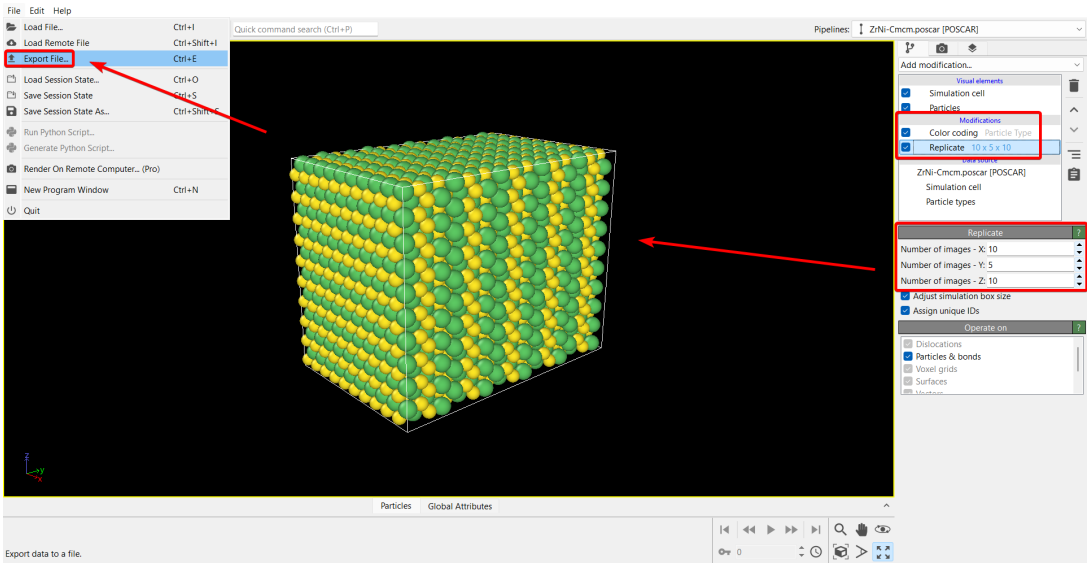

Figure 8: Replication procedure and export.

These files, stored in the `'Structure'` folder, are essential for the input preparation in the simulations, ensuring that the bulk configurations is available for accurate modeling of the Ni-Zr alloys.

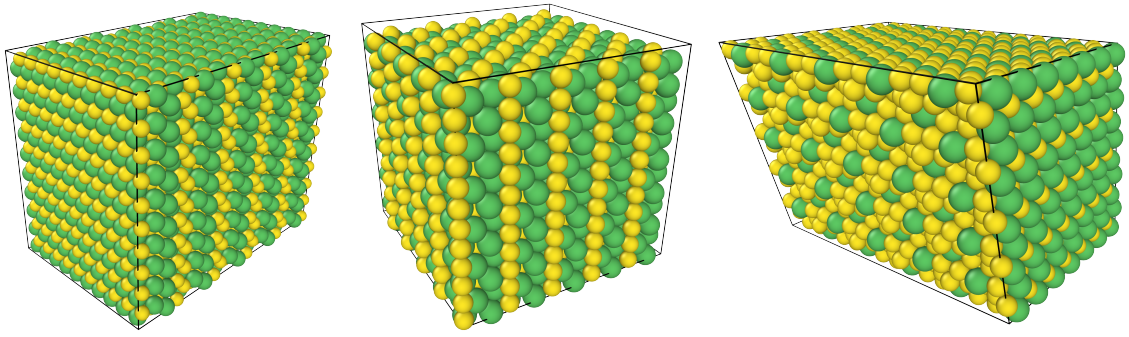

(a) ZrNi **(b)** Zr_2Ni **(c)** Zr_2Ni_7

Figure 9: Ni-Zr compounds in OVITO where Zr is green and Ni is yellow.

2.3 Melting Approach for Alloys

The approach adopted for the alloy simulations is the **two-phase coexistence method** [18,19]. This method is a cornerstone of computational thermodynamics for evaluating phase stability and transition temperatures, especially in complex alloy systems.

The melting temperature of a material is defined as the temperature at which its solid and liquid phases coexist in equilibrium. In MD simulations, achieving such equilibrium requires

carefully balancing thermodynamic and structural factors. The two-phase coexistence method was chosen due to its ability to directly simulate the interplay between the two phases without relying on approximations or extrapolations.

Compared to other computational techniques, such as the overheating method or free-energy-based approaches, the two-phase method offers several advantages:

a. By simulating both phases within the same system, this method provides a clear visual and quantitative distinction between solid and liquid regions.

b. It accurately captures the melting point as the temperature where neither phase grows or diminishes over time, reflecting true equilibrium.

c. For multicomponent systems like Ni-Zr, where complex phase interactions occur, this method avoids the need for analytical free-energy functions, which are often difficult to parameterize.

The simulation workflow for determining the melting temperature involved the following steps:

1) Initialization and Relaxation
The starting structure consisted of a bulk solid phase, derived from crystallographic data of the target Ni-Zr composition (e.g., ZrNi, Zr_2Ni, Zr_2Ni_7).
The structure was relaxed at 0 K to eliminate residual stresses and ensure that the system was in its lowest-energy configuration, in order to minimized inaccuracies stemming from unrealistically distorted initial configurations.

2) Creation of the Two-Phase System
A liquid region was created by melting a portion of the solid structure at a high temperature (typically well above the expected melting point).
The system was then equilibrated to ensure a distinct interface between the solid and liquid phases. This interface plays a critical role in determining the stability of each phase during subsequent simulations.

3) Thermal Equilibration
The two-phase system was equilibrated at various test temperatures using an NPT ensemble.
The simulation box was allowed to expand or contract isotropically, enabling the system to reach equilibrium without imposing artificial constraints.

4) Phase Behaviour Analysis
Below the melting point, the liquid phase recrystallized into the solid phase.
Above the melting point, the solid phase melted into the liquid phase.
At the melting point, both phases remained stable over time.

5) Data Collection and Interpretation

Thermodynamic properties (e.g., temperature, pressure, volume, total energy) were logged throughout the simulations. Also, atomic configurations were periodically saved for visualization and analysis, enabling the identification of phase boundaries and transitions.

The full script used for these simulations (file name `in.ZrNi-melting_phase`) is provided below for reference; each section of the script corresponds to the steps outlined above.

```
# Luigi Casagrande
echo            none

# LAMMPS Code
units           metal
boundary        p p p
atom_style      atomic

# Raw data from the material
read_data       ../Relaxed_Structure/ZrNi-Cmcm_relaxed.dat

# Target test Temperature and Pressure
variable        temperature equal 1533.0 # Kelvin
variable        pressure equal 1.0 # bar

# Alloy potential
pair_style      eam/fs
pair_coeff      * * ../Ni-Zr.eam.fs Ni Zr

# Log file output
variable        cohesive equal etotal/atoms
variable        atomicVolume equal vol/atoms
thermo_style    custom step time temp etotal v_cohesive press vol
   v_atomicVolume

# NVT dynamics
region          liquidRegion block INF INF INF INF 0 INF
group           liquid region liquidRegion
region          solidRegion block INF INF INF INF INF 0
group           solid region solidRegion

fix             nvtFix   liquid   nvt temp 1700.0 1700.0 $(100.0 * dt)
velocity        liquid create 1700.0 123456 dist gaussian
fix             freezeFix solid    setforce 0.0 0.0 0.0
fix             recenterFix all      recenter INIT INIT INIT
dump            twoPhase all      atom 5000 ../Output/ZrNi-
   two_phase_creation.dump
reset_timestep  0

run             50000
unfix           nvtFix
unfix           freezeFix
unfix           recenterFix
undump          twoPhase

# Variables for thermodynamic outputs
```

```
45 variable         step equal step
46 variable         temp equal temp
47 variable         vol equal vol
48 variable         Et equal etotal
49 variable         press equal press
50
51 # Specify thermodynamic style for periodic log updates
52 thermo_style     custom step time temp etotal press vol
53
54 # Thermal properties output during NPT equilibration
55 fix              printThermal all      print 1000 "${step} ${temp} ${vol
      } ${Et} ${press}" file ../Simulation_Data/ZrNi_melting.dat screen no
56
57 # NPT dynamics
58 fix              nptFix   all      npt temp ${temperature} ${temperature
      } $(100.0*dt) iso ${pressure} ${pressure} $(1000.0*dt)
59 fix              recenterFix all      recenter INIT INIT INIT
60 dump             equilibration all      atom 5000 ../Output/ZrNi-
      equilibration.dump
61 reset_timestep  0
62
63 run              500000
64 unfix            nptFix
65 undump           equilibration
66 unfix            recenterFix
```

To facilitate understanding of the methodology, it is necessary to further clarify the following LAMMPS commands used in the simulation, particularly in the NVT and NPT dynamics stages.

- **NVT Dynamics**

  > `region liquidRegion block INF INF INF INF 0 INF`
  Defines a region in the simulation box named `liquidRegion`, extending infinitely in the x and y directions, but confined to the positive z-axis ($z > 0$), specifying the spatial domain that will represent the liquid phase.

  > `group liquid region liquidRegion`
  Assigns all atoms within the `liquidRegion` to a group called `liquid`. This enables targeted operations, such as applying specific fixes or dynamics to this subset of atoms.

  > `region solidRegion block INF INF INF INF INF 0`
  Creates a region named `solidRegion`, which is confined to the negative z-axis ($z < 0$), representing the solid phase in the simulation.

  > `group solid region solidRegion`
  Assigns atoms within the `solidRegion` to a group named `solid`. Like the liquid group, this allows independent manipulation of the solid-phase atoms.

> `fix nvtFix liquid nvt temp 1700.0 1700.0 $(100.0 * dt)`
Applies an NVT ensemble to the `liquid` group. This ensures constant number of particles, volume, and temperature for the liquid region. The system is initialized and equilibrated at a temperature way above the melting point (in the case of ZrNi, 1700 K) using a Nose-Hoover thermostat, with a temperature damping time of `100*dt` (time steps).

> `velocity liquid create 1700.0 123456 dist gaussian`
Generates random initial velocities for the atoms in the `liquid` group, consistent with a Maxwell-Boltzmann distribution at 1700 K. The random seed `123456` ensures reproducibility every time the simulation runs.

> `fix freezeFix solid setforce 0.0 0.0 0.0`
Freezes the motion of atoms in the `solid` group by setting their net force components in the x, y, and z directions to zero. This maintains the structural integrity of the solid region during liquid equilibration.

> `fix recenterFix all recenter INIT INIT INIT`
Keeps the center of mass of the entire system (`all` group) fixed at its initial position (`INIT INIT INIT`) during the simulation. This prevents spurious drifts caused by thermal fluctuations or numerical instabilities.

- **NPT Dynamics**

> `fix nptFix all npt temp $temperature $temperature $(100.0*dt) iso $pressure $pressure $(1000.0*dt)`
Applies an NPT ensemble to the entire system (`all` group). This maintains constant number of particles, pressure, and temperature, allowing the simulation box dimensions to fluctuate isotropically to maintain the specified pressure. The thermostat and barostat damping times are set to `100*dt` and `1000*dt`, respectively, to ensure gradual equilibration.

> `fix recenterFix all recenter INIT INIT INIT`
Re-centers the entire system's center of mass at its initial position during the NPT dynamics stage, ensuring stability and eliminating translational motion of the system as a whole.

2.4 Melting Approach for Pure Metals

The approach employed for determining the melting temperature of pure metals differs fundamentally from the two-phase coexistence method outlined in section 2.3.
Here, the melting point is determined by **gradually heating** the material from its solid state to its liquid state in a controlled simulation. The process involves monitoring

changes in thermodynamic and structural properties, particularly the volume-temperature relationship. The melting temperature is identified as the point of discontinuity in the $V - T$ curve, where a sudden increase in volume indicates the phase transition from solid to liquid.

This method offers a straightforward and computationally efficient alternative to more elaborate techniques like the two-phase coexistence method. Unlike the latter, which requires the preparation and equilibration of separate solid and liquid phases within the same simulation, the direct heating approach simplifies the setup and execution. Furthermore, it is particularly advantageous when working with pure metals, where the transition between solid and liquid phases tends to be sharp and well-defined, making the melting point easier to pinpoint.

The script for pure Ni (file name `'in.Ni-melting'`) is as follows:

```
# Luigi Casagrande
echo none

# Initialize LAMMPS
units           metal
boundary        p p p
atom_style      atomic

timestep        0.001

read_data       Ni-Fm-3m

pair_style      eam/fs
pair_coeff      * * ../Ni.eam.fs Ni

# Initial Temp and velocity is 10K, initial Pressure is 1
variable        step equal step
variable        time equal step*dt
variable        temp equal temp
variable        vol equal vol
variable        Et equal etotal
variable        press equal press*0.1 # in[Mpa] unit for pressure

variable        Tstart equal 10 # Start T
variable        Tdamp equal 8000*dt # Temperature damping parameter for
    thermostat
variable        Pdamp equal 100*dt # Pressure damping parameter for
   barostat
variable        Tstop equal 1900 # Stop T
velocity        all create ${Tstart} 1234567 # Velocity initialization

compute         pea      all      pe/atom
compute         kea      all      ke/atom

thermo          1000
thermo_style    custom step temp vol v_Et pe ke press

# Equilibration run
```

```
dump            1       all     custom 10000 ../Output/Ni-equilibration_melting.xyz id type x y z c_pea c_kea
fix             1       all     npt temp ${Tstart} ${Tstart} ${Tdamp} iso 0 0 ${Pdamp}
run             10000
unfix           1
undump          1

# Heating from initial Tstart to Tstop
reset_timestep  0

dump            1       all     custom 10000 ../Output/Ni_melting.xyz id type x y z c_pea c_kea #c_csp
fix             print   all     print 1000 "${step} ${temp} ${vol} ${Et} ${press}" file ../Simulation_Data/Ni_melting_v1.dat
fix             1       all     npt temp ${Tstart} ${Tstop} ${Tdamp} iso 0 0 ${Pdamp}

run             1000000
unfix           1
undump          1
```

Also in this case, in order to facilitate understanding of the methodology, it is necessary to clarify the following LAMMPS commands:

- `variable Tdamp equal 8000*dt` and `variable Pdamp equal 100*dt`
  Define the time constants for adjusting temperature and pressure, ensuring smooth thermal equilibration and regulating volume change for isotropic pressure control.

- `fix 1 all npt temp $Tstart $Tstart $Tdamp iso 0 0 $Pdamp`
  Applies an NPT ensemble to maintain constant temperature (`Tstart`) and pressure (`0` in all directions). `Tdamp` controls how quickly the system reaches the target temperature, and `Pdamp` sets the damping time for pressure fluctuations.

- `compute pea all pe/atom` and `compute kea all ke/atom`
  Calculate potential energy (`pe/atom`) and kinetic energy (`ke/atom`) for each atom, enabling detailed energy analysis.

- `thermo_style custom step temp vol v_Et pe ke press`
  Defines the thermodynamic properties to output: simulation step, temperature, volume, total energy (`v_Et`), potential energy, kinetic energy, and pressure.

2.5 MATLAB Analysis

The following MATLAB script is designed to analyze the output data from the LAMMPS simulations presented in sections 2.3 and 2.4 to determine the melting temperature of the material.
The approach involves plotting thermodynamic properties as functions of temperature

and identifying characteristic changes in these properties.
The melting temperature corresponds to the point where significant shifts occur, indicative of a phase transition from solid to liquid.

In particular during a phase transition, the system's volume typically exhibits a distinct, sharp change. The script calculates the derivative of volume with respect to temperature ($\mathrm{d}V/\mathrm{d}T$) to pinpoint this transition. The same idea is then applied to the energy with respect to temperature. Both analyses are complementary, providing robust confirmation of the melting temperature.

Key parts of the code (file name `'Melting_Temperature.m'`) include:

- **Data Extraction:**

```
filename = '...';
data = readmatrix(filename, 'CommentStyle', '#');
step = data(:,1);    % Step
temp = data(:,2);    % Temperature
vol = data(:,3);     % Volume
Et = data(:,4);      % Total energy
press = data(:,5);   % Pressure
```

  where the file will be picked from the `'Simulation_Data'` folder.

- **Volume-Temperature Plot and Analysis:**

```
plot(temp, vol, 'b-', 'LineWidth', 2);
dVdT = diff(vol) ./ diff(temp); % First derivative (dV/dT)
dVdT = [dVdT(1); dVdT]; % Add the first element back to maintain
    the same length
[~, idx_melting] = max(dVdT); % Index of maximum derivative
celsius1 = temp(idx_melting) - 273.15;
```

  The script finds the index of the maximum $\mathrm{d}V/\mathrm{d}T$ and retrieves the corresponding temperature. This temperature represents the melting point and is printed both in Kelvin and Celsius.

- **Energy-Temperature Plot and Analysis:**

```
plot(temp, Et, 'g-', 'LineWidth', 2);
dEdT = diff(Et) ./ diff(temp); % First derivative (dE/dT)
dEdT = [dEdT(1); dEdT]; % Add the first element back to maintain
    the same length
[~, idx_melting_energy] = max(dEdT); % Index of maximum derivative
celsius2 = temp(idx_melting_energy) - 273.15;
```

  The same principle as the previous point is applied for the energy analysis.

- **Output and Interpretation:**

```
fprintf('Melting Temperature (from dV/dT analysis):\n%.2f K = %.2f
    °C\n', temp(idx_melting), celsius1);
fprintf('Melting Temperature (from dE/dT analysis):\n%.2f K = %.2f
    °C\n', temp(idx_melting_energy), celsius2);
```

These results are compared for consistency.

The complete code (file name '`Melting_Temperature.m`') is the following:

```
%% Luigi Casagrande
clc;
close all;
clear;

%% LAMMPS data extraction
% Format: Step, Temperature, Volume, Total Energy, Pressure
filename = 'Simulation_Data\ZrNi_melting.dat';
data = readmatrix(filename, 'CommentStyle', '#');

step = data(:,1);    % Step
temp = data(:,2);    % Temperature
vol = data(:,3);     % Volume
Et = data(:,4);      % Total energy
press = data(:,5);   % Pressure

%% Plot Volume - Temperature
% SubPlot V - T
figure(1);
set(gcf, 'Position', [50, 150, 650, 600]);
subplot(2,1,1);
plot(temp, vol, 'b-', 'LineWidth', 2);
title('Volume vs. Temperature (V - T)');
xlabel('Temperature (K)');
ylabel('Volume (Å^3)');
grid on;

% Derivative of volume with respect to temperature
dVdT = diff(vol) ./ diff(temp); % First derivative (dV/dT)
dVdT = [dVdT(1); dVdT]; % Add the first element back to maintain the
    same length

% SubPlot dV/dT - T
subplot(2,1,2);
plot(temp, dVdT, 'r-', 'LineWidth', 2);
title('Derivative of Volume with respect to Temperature (dV/dT - T)');
xlabel('Temperature (K)');
ylabel('dV/dT (Å^3/K)');
grid on;

% Identify the melting point from dV/dT plot - sharp peak/change
[~, idx_melting] = max(dVdT); % Index of maximum derivative
celsius1 = temp(idx_melting) - 273.15;

% Melting temperature (from the V-T plot) output
fprintf('Melting Temperature (from dV/dT analysis):\n%.2f K = %.2f °C\n'
    , temp(idx_melting), celsius1);

%% Plot Energy - Temperature
% SubPlot Et - T
figure(2);
set(gcf, 'Position', [730, 150, 650, 600]);
```

```
51 subplot(2,1,1);
52 plot(temp, Et, 'g-', 'LineWidth', 2);
53 title('Total Energy vs. Temperature (Et - T)');
54 xlabel('Temperature (K)');
55 ylabel('Total Energy (eV)');
56 grid on;
57
58 % Derivative of total energy with respect to temperature
59 dEdT = diff(Et) ./ diff(temp);
60 dEdT = [dEdT(1); dEdT]; % Add the first element back to maintain the
       same length
61
62 % SubPlot dE/dT - T
63 subplot(2,1,2);
64 plot(temp, dEdT, 'm-', 'LineWidth', 2);
65 title('Derivative of Total Energy with respect to Temperature (dE/dT -
       T)');
66 xlabel('Temperature (K)');
67 ylabel('dE/dT (eV/K)');
68 grid on;
69
70 % The melting point is typically where dE/dT shows a sharp increase.
71 [~, idx_melting_energy] = max(dEdT); % Index of maximum derivative
72 celsius2 = temp(idx_melting_energy) - 273.15;
73
74 fprintf('Melting Temperature (from dE/dT analysis):\n%.2f K = %.2f °C\n'
       , temp(idx_melting_energy), celsius2);
```

3 Results

3.1 ZrNi Alloy

The MATLAB analysis yielded the following graphs illustrating the Volume-Temperature ($V-T$) and Energy-Temperature ($E-T$) relationships for the ZrNi alloy. The simulation spanned the temperature range of 1100 to 1600 K, with a focus on identifying the melting point. The melting point is determined by the peaks in the derivative graphs ($\mathrm{d}V/\mathrm{d}T$ and $\mathrm{d}E/\mathrm{d}T$), which signify the sharpest changes in volume and energy associated with the phase transition.

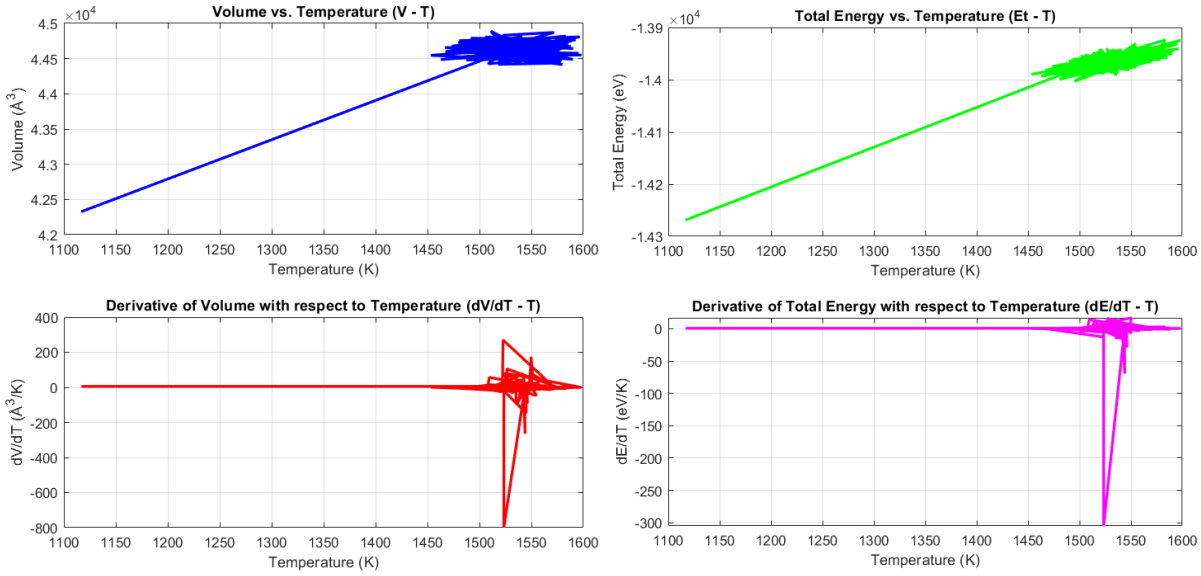

(a) **(b)**

Figure 10: Plots obtained from the MATLAB simulation for ZrNi alloy.

The results from the analysis indicate melting temperatures of 1249.49 °C (derived from the volume derivative) and 1277.19 °C (derived from the energy derivative).

```
> Melting Temperature (from dV/dT analysis): 1522.64 K = 1249.49 °C
> Melting Temperature (from dE/dT analysis): 1550.34 K = 1277.19 °C
```

The results of the LAMMPS simulations were further analyzed through OVITO to visually inspect the atomic configurations and phase behaviours at critical stages, to ensure and verify the correct functioning of the script. Two key outputs, `'two_phase_creation'` and `'equilibration'` are obtained from the script shown in section 2.3.

The two-phase creation file (`'ZrNi-two_phase_creation.dump'`) illustrates the initial setup of the system, showing a solid phase (atoms ordered, $z < 0$) and a liquid phase (atoms disordered, $z > 0$). This visual clearly highlights the coexistence of the two phases, as shown in Figure 11.

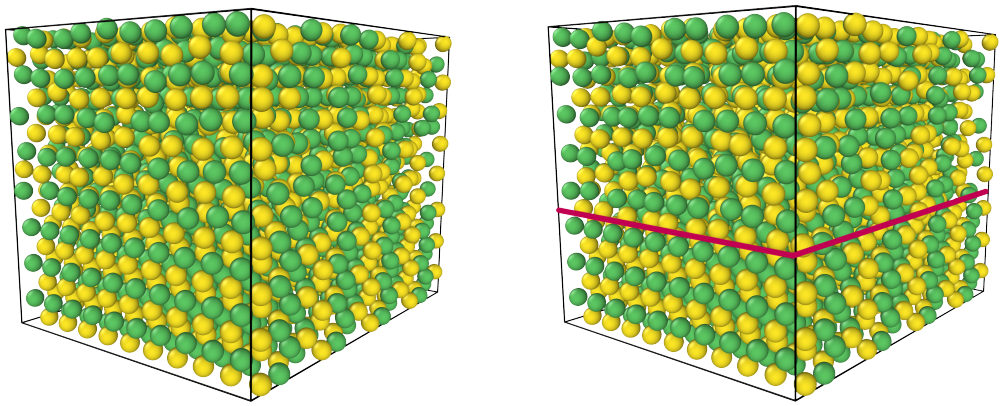

(a) Frame 1 **(b)** Frame 2

Figure 11: ZrNi two-phase creation, where the red line indicates $z = 0$.

The equilibration file (`'ZrNi-equilibration.dump'`) captures the atomic configurations during the simulations around the melting point, showcasing the dynamic interplay between solid and liquid regions as the system stabilizes near equilibrium.

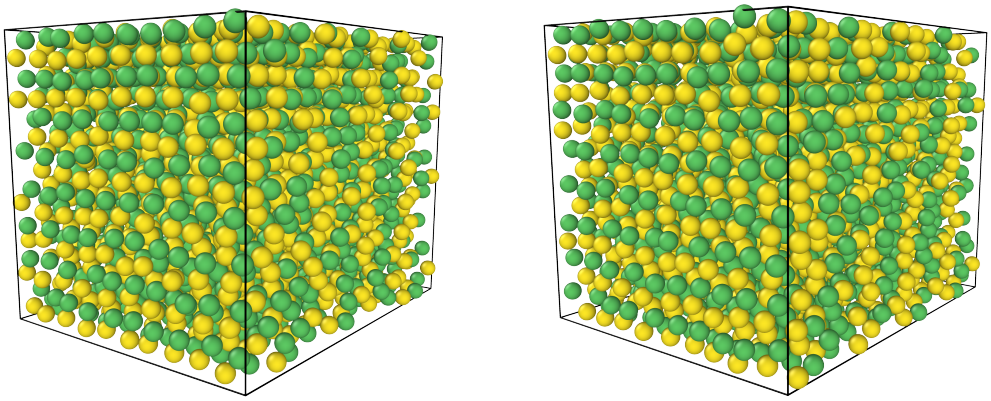

(a) Frame 35 **(b)** Frame 36

Figure 12: ZrNi equilibration output.

3.2 Zr_2Ni Alloy

For the Zr_2Ni alloy, the MATLAB analysis followed the similar procedure, with simulations performed over the temperature range of 950 to 1450 K. In the same way, the melting point was identified by examining the $V - T$ and $E - T$ derivative graphs, where the peaks indicate the transition from solid to liquid phases.

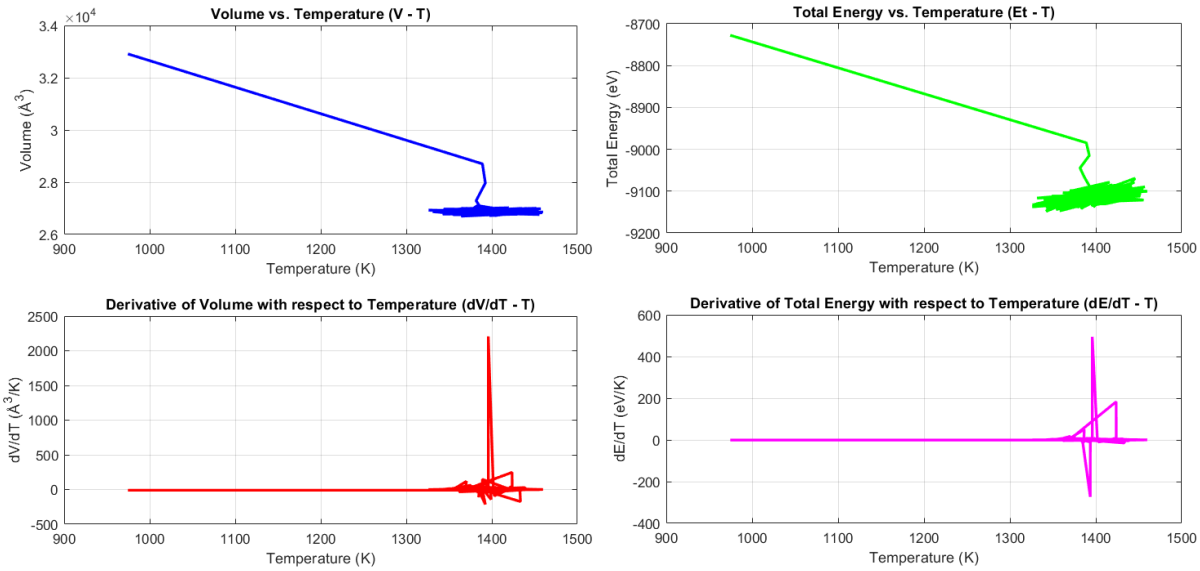

(a) **(b)**

Figure 13: Plots obtained from the MATLAB simulation for Zr_2Ni alloy.

The melting temperatures obtained are 1122.68 °C from the volume analysis and 1122.68 °C from the energy analysis.

```
> Melting Temperature (from dV/dT analysis): 1395.83 K = 1122.68 °C
> Melting Temperature (from dE/dT analysis): 1395.83 K = 1122.68 °C
```

In the same way, the OVITO results are:

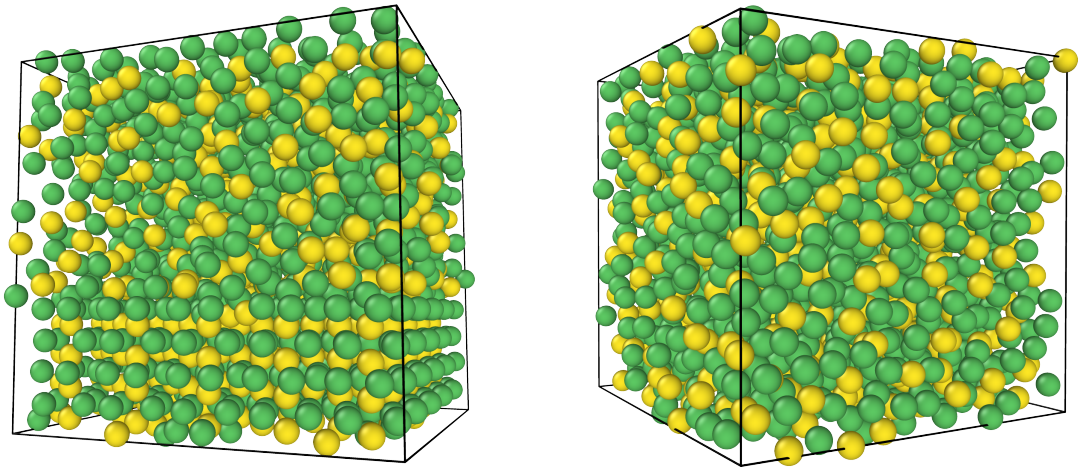

(a) Zr_2Ni two-phase creation **(b)** Zr_2Ni equilibration output

Figure 14: Output for Zr_2Ni alloy.

3.3 Zr_2Ni_7 Alloy

The Zr_2Ni_7 alloy was analyzed in the same manner as the other compounds, with a focus on detecting phase transition behaviour within the temperature range of 1600 to 2000 K approximately. The derivative graphs of $V-T$ and $E-T$ reveal multiple peaks that will be addressed in section 4.1.

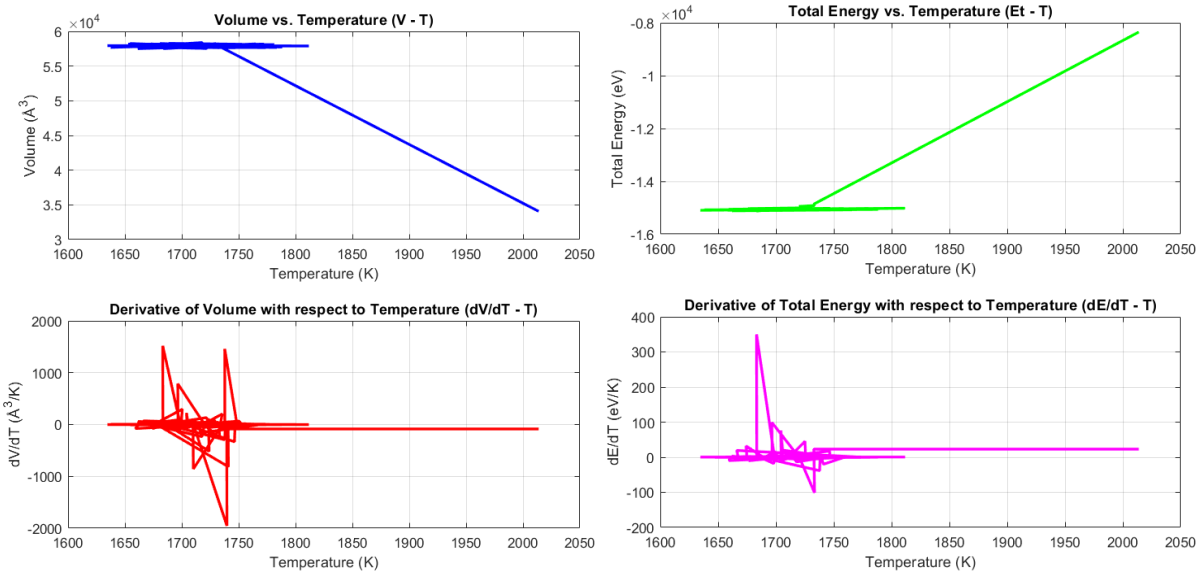

(a) **(b)**

Figure 15: Plots obtained from the MATLAB simulation for Zr_2Ni_7 alloy.

From the analysis, the melting temperatures were determined as 1410.08 °C from the volume derivative and 1410.08 °C from the energy derivative.

```
> Melting Temperature (from dV/dT analysis): 1683.23 K = 1410.08 °C
> Melting Temperature (from dE/dT analysis): 1683.23 K = 1410.08 °C
```

3.4 Pure Ni

The melting behaviour of pure Ni was analyzed using the two potential files, `'Ni_v1.eam.fs'` and `'Ni_v2.eam.fs'`. The $V-T$ and $E-T$ plots for each case were generated to identify the melting temperature by observing distinct changes in these curves.

For the first potential file (`'Ni_v1.eam.fs'` in Figure 16a), the $V-T$ plot shows a nearly linear increase in volume with temperature, as expected during heating in the solid phase. However, at 1535.75 K, there is a notable discontinuity where the slope changes significantly, indicating the melting transition.

Using the updated and refined potential file (`'Ni_v2.eam.fs'` in Figure 16b), the $V-T$ and $E-T$ curves show more accurate behaviour. The melting point was identified at 1726.97 K.

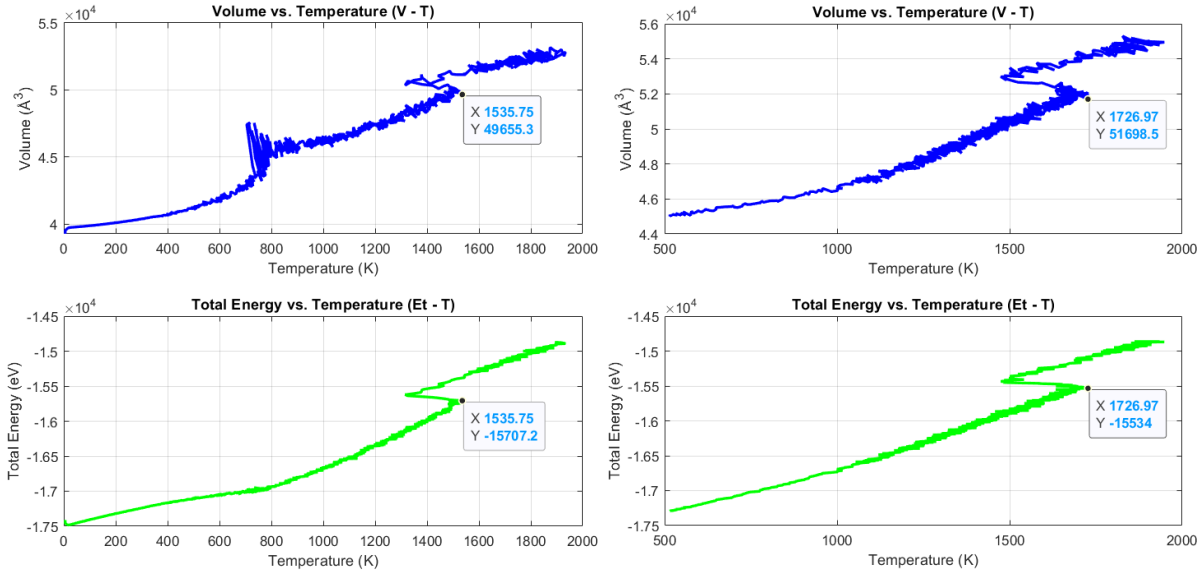

(a) Potential file `v1` **(b)** Potential file `v2`

Figure 16: Plots obtained from the MATLAB simulation for pure Ni.

3.5 Pure Zr

For pure Zn, the melting behaviour was evaluated using a single potential file, and the $V-T$ and $E-T$ plots were analyzed similarly. The $V-T$ curve shows a linear volume increase during heating, with a pronounced discontinuity at 2125.12 K, marking the transition from the solid to liquid phase.

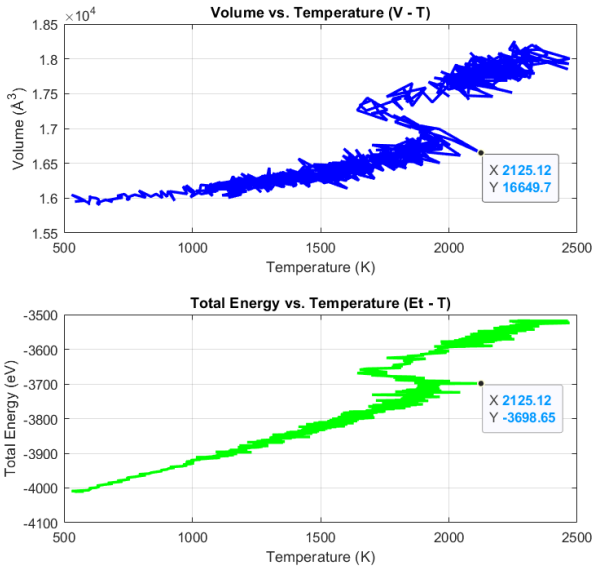

Figure 17: Plots obtained from the MATLAB simulation for pure Zr.

4 Discussion

4.1 Ni-Zr Alloys

The melting temperature data obtained from the simulations are summarized in Table 1, where two independent estimates (from volume-temperature and energy-temperature analyses) are averaged for each alloy.

Table 1: Summary of the results seen in section 3.

Alloy	V-T [°C]	E-T [°C]	Average [°C]
ZrNi	1249.49	1277.19	1263.34
Zr_2Ni	1122.68	1122.68	1122.68
Zr_2Ni_7	1410.08	1410.08	1410.08

A comparison with experimental/reference data is provided in the following table.

Table 2: Comparison with the real data shown in Figure 4.

Alloy	Average [°C]	Real Data [°C]	Error [%]
ZrNi	1263.34	1260	+0.27
Zr_2Ni	1122.68	1120	+0.24
Zr_2Ni_7	1410.08	1438	−1.94

The results for ZrNi and Zr_2Ni show excellent agreement with experimental values, reflecting the accuracy of the potential model used. This precision is expected since the `EAM/fs` potential was specifically developed to simulate these two phases, ensuring reliable predictions for their thermal behaviour.

In contrast, the Zr_2Ni_7 alloy exhibits a more significant deviation from experimental values. This discrepancy likely arises from the fact that the potential was not optimized for this phase, resulting in less accurate interatomic interactions for Zr_2Ni_7.

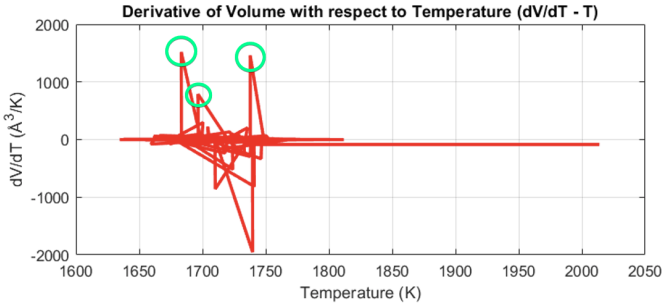

Figure 18: From Figure 15a, multiple peaks can be observed in the Zr_2Ni_7 data analysis.

The derivative graphs for this alloy reveal multiple peaks (Figure 15) instead of a single distinct one (such as the one in Figure 13).
These additional peaks indicate competing transitions or localized phase instabilities, suggesting that the melting process is less straightforward, possibly due to a complex interplay of structural rearrangements.

For ZrNi, the melting temperatures derived from $V - T$ and $E - T$ analyses differ slightly. This divergence can arise from the sensitivity of each method to different physical phenomena.
The volume-temperature analysis primarily captures structural changes, while the energy-temperature analysis reflects the energetic stability of phases. Despite this variation, their average aligns well with the experimental melting temperature.
This agreement can be attributed to the robustness of the two-phase coexistence method, which averages out inconsistencies and ensures a reliable estimate.

4.2 Pure Ni and Zr

The simulation results for the melting points of pure Ni and Zr demonstrate a high degree of accuracy, highlighting the reliability of the computational approach and the potentials employed.

Table 3: Comparison with the real data shown in Figure 4.

Element	Simulation [°C]	Real Data [°C]	Error [%]
Ni	1453.82	1455	−0.08
Zr	1851.97	1855	−0.16

For Ni, the calculated melting temperature is 1453.82 °C, closely matching the experimental value of 1455 °C. The negligible deviation of 1.18 °C can be attributed to the accuracy of the `'Ni_v2.eam.fs'` potential, which has been specifically refined for precise thermal property modeling, including the melting phenomenon.
The `v1` potential file yields a melting temperature of 1262.60 °C, which is significantly lower than experimental data. This discrepancy suggests that the `v1` potential was not adequately optimized for simulations involving melting behaviour.

Similarly, for Zr, the simulated melting point of 1851.97 °C aligns well with the experimental value of 1855 °C, yielding a deviation of only 3.03 °C.

The slight deviations for both materials can be attributed to minor numerical artifacts, such as the finite simulation time, heating rates, or limitations in the interatomic potential parameterization at high temperature conditions.

5 Conclusion

The results obtained from the simulation on LAMMPS demonstrate a high level of accuracy, with calculated melting temperatures closely aligned with experimental data. The success of the simulations highlights the reliability of both the computational methods and interatomic potentials employed.
Notably, the deviations observed are minimal and within acceptable margins, underscoring the robustness of molecular dynamics as a predictive tool for studying thermal properties in metals and alloys.
These findings further validate the approach and offer insights for future investigations into phase transitions and material behaviour at high temperatures.

As seen, the choice of an appropriate potential file is crucial in MD simulations, as it directly impacts the accuracy of the predicted material properties.
An improperly chosen or non-optimized potential can lead to significant deviations from experimental data, undermining the reliability of the simulation results.

References

[1] Michael Dayah. *Periodic table*. 2024. URL: `https://ptable.com/`.

[2] Anubhav Jain et al. "Commentary: The Materials Project: A materials genome approach to accelerating materials innovation". In: *APL materials* 1.1 (2013).

[3] Alejandro N Filippin et al. "Ni–Al–Cr superalloy as high temperature cathode current collector for advanced thin film Li batteries". In: *RSC advances* 8.36 (2018), pp. 20304–20313.

[4] Zhengang Duan et al. "Current status of materials development of nuclear fuel cladding tubes for light water reactors". In: *Nuclear Engineering and Design* 316 (2017), pp. 131–150.

[5] Ramagonolla Kranthikumar and Yoshito Kishi. "Application of Ni/Zr-Mediated Ketone Coupling for the Scalable Synthesis of Homohalichondrin B". In: *Organic Letters* 26.34 (2024), pp. 7105–7109.

[6] Mahwash Mahar Gul et al. "NiZr2S4 bimetallic sulphide thin films: synthesis and multifunctional applications in nanotechnology". In: *Journal of Applied Electrochemistry* 54.7 (2024), pp. 1667–1681.

[7] Abdel F Isakovic et al. "Structural, Transport, and Magnetic Characterization of NiZr Metallic Glasses with varied Ni/Zr composition". In: *MRS Online Proceedings Library (OPL)* 1300 (2011), mrsf10–1300.

[8] Tianyi Ma et al. "Experimental Investigation of Phase Equilibria in the Cr-Ni-Zr Ternary System". In: *Journal of Phase Equilibria and Diffusion* 43.6 (2022), pp. 780–791.

[9] *Alloy Phase Diagram Database (ASM)*. en. URL: https://matdata.asminternational.org/apd/index.aspx?search=Nickel-Zirconium+Binary+Phase+Diagram+%282007+Wang+N.%29 (visited on 11/25/2024).

[10] P Nash and CS Jayanth. "The Ni-Zr (nickel-zirconium) system". In: *Bulletin of Alloy Phase Diagrams* 5.2 (1984), pp. 144–148.

[11] Na Wang et al. "Experimental study and thermodynamic re-assessment of the Ni–Zr system". In: *Calphad* 31.4 (2007), pp. 413–421.

[12] SR Wilson and MI Mendelev. "Anisotropy of the solid–liquid interface properties of the Ni–Zr B33 phase from molecular dynamics simulation". In: *Philosophical Magazine* 95.2 (2015), pp. 224–241.

[13] MI Mendelev et al. "Development of interatomic potentials appropriate for simulation of liquid and glass properties of NiZr2 alloy". In: *Philosophical Magazine* 92.35 (2012), pp. 4454–4469.

[14] MW Finnis and JE Sinclair. "A simple empirical N-body potential for transition metals". In: *Philosophical Magazine A* 50.1 (1984), pp. 45–55.

[15] *1987–Ackland-G-J-Tichy-G-Vitek-V-Finnis-M-W–Ni*. en. URL: https://www.ctcms.nist.gov/potentials/entry/1987--Ackland-G-J-Tichy-G-Vitek-V-Finnis-M-W--Ni/ (visited on 11/29/2024).

[16] Mikhail I Mendelev and Graeme J Ackland. "Development of an interatomic potential for the simulation of phase transformations in zirconium". In: *Philosophical Magazine Letters* 87.5 (2007), pp. 349–359.

[17] *2007–Mendelev-M-I-Ackland-G-J–Zr-1*. en. URL: https://www.ctcms.nist.gov/potentials/entry/2007--Mendelev-M-I-Ackland-G-J--Zr-1/ (visited on 11/29/2024).

[18] James R Morris et al. "Melting line of aluminum from simulations of coexisting phases". In: *Physical Review B* 49.5 (1994), p. 3109.

[19] C Cazorla et al. "Ab initio melting curve of molybdenum by the phase coexistence method". In: *The Journal of chemical physics* 126.19 (2007).